SAND2011-3914C

ULTRATHIN FLEXIBLE CRYSTALLINE SILICON: MICROSYSTEMS ENABLED PHOTOVOLTAICS

Jose L. Cruz-Campa, Gregory N. Nielson, Paul J. Resnick, Carlos A. Sanchez,
Peggy J. Clews, Murat Okandan, Tom Friedmann, Vipin Gupta
Sandia National Laboratories, Albuquerque, NM, USA

ABSTRACT

We present an approach to create ultrathin (<20 µm) and highly flexible crystalline silicon sheets on inexpensive substrates. We have demonstrated silicon sheets capable of bending at a radius of curvature as small as 2 mm without damaging the silicon structure. Using microsystem tools, we created a suspended sub-millimeter honeycomb segmented silicon structure anchored to the wafer only by small tethers. This structure is created in a standard thickness wafer enabling compatibility with common processing tools. The procedure enables all the high temperature steps necessary to create a solar cell to be completed while the cells are on the wafer. In the transfer process, the cells attach to an adhesive flexible substrate which, when pulled away from the wafer, breaks the tethers, and releases the honeycomb structure.

We have previously demonstrated that sub mm and ultrathin silicon segments can be converted into highly efficient solar cells, achieving efficiencies up to 14.9% in thicknesses of 14 µm. With this technology, achieving high-efficiency (>15%) and highly flexible PV modules should be possible.

INTRODUCTION

Reducing the thickness of crystalline silicon wafers has been a long term goal in the solar industry. As of 2010, most of the silicon solar cell companies were working with 6 inch wafers with thicknesses between 180 and 200 µm. In addition, a significant portion of the crystalline silicon material is lost during sawing. The effective material usage is equivalent to a wafer with a thickness of 310-475 µm depending on the thickness of the saw wire. Although there is a strong cost driver to use thinner wafers, handling wafers thinner than 180 µm is challenging while maintaining adequate yield. Another problem with thin wafers is the need for higher quality passivation. Due to the closer proximity of surfaces to collection points in thin wafers, well passivated surfaces are crucial for high efficiencies.

Microsystems Enabled Photovoltaics (MEPV) is a technique to create solar cells relying on tools and techniques from the microsystems and integrated circuit (IC) industry [1]. The use of these tools could improve yield, efficiency, and uniformity of solar cells with a mature and scalable material base and processing know-how. Other groups around the world have taken advantage of these techniques to produce small and thin solar cells [2, 3].

In previous efforts [4,5], our group produced functional ultrathin silicon solar cells. Their size ranged from 250 µm to 10 mm in diameter with a thickness range of 14 to 20 µm. Fig. 1 shows a scanning electron microscope (SEM) picture of a 1 mm, back contacted, crystalline silicon solar cell with interdigitated radial contacts. Throughout our research, it was seen that one of the most critical parameters for high efficiency in these ultrathin structures is surface passivation. The process on the first generation of cells was only capable of passivating the back side of the cell, leaving the front side unpassivated. Further processing of the cell after release was needed to create a front passivation layer. After optimization of designs and passivation techniques, we were able to obtain efficiencies as high as 14.9% in thicknesses as thin as 14 µm [6].

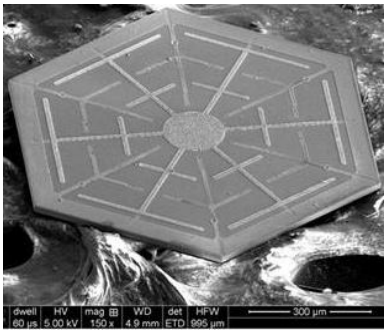

Figure 1 SEM picture of a 1 mm diameter, 20 µm thick solar cell produced with microsystem tools.

Passivating the front of MEPV cells after release is challenging and cannot be done with standard processing tools. Thus, here we present a design capable of performing full passivation while the cell is still attached to the wafer. The basic idea is to have the cell anchored to the substrate through very small tethers. The tethers leave a gap between the front of the cell and the substrate and a thin layer of nitride or oxide can be grown on the surfaces while the cell is still attached to the substrate. Fig. 2 shows a sketch of the proposed cell attached to the substrate through the tethers (anchors).

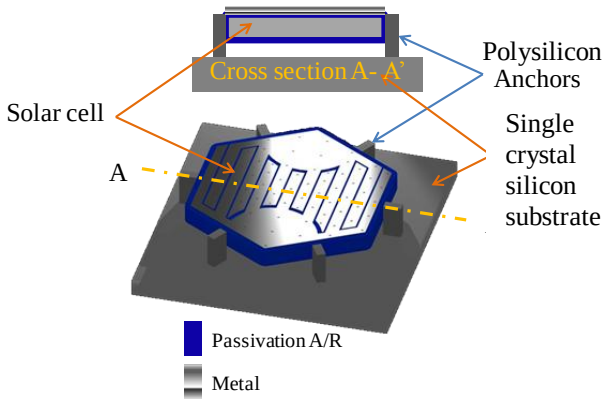

Figure 2 Suspended solar cell design that enables full passivation while still attached to the wafer.

DESIGN

Mechanical analysis provided guidance on the design limitations with respect to different variables: cell size, buried oxide thickness, stresses caused by capillary forces, the tape release forces, etc.

First, capillary forces were calculated. Then, the stress in the tethers caused by capillary forces was calculated to see if it did not exceed the maximum stress allowed for fracture in silicon. Using the capillary force again, the deflection on the cell was calculated: if the deflection was larger than the gap between the cell and the substrate, the cell would stick to the substrate.

To calculate the force between the cell and the substrate due to capillary forces, the equation for two parallel plates made of the same material with liquid in between was used [7]. Water @ 25 °C was assumed to be the liquid in between the substrate and the cell. Fig. 3 shows the parameters in the calculation of capillary forces.

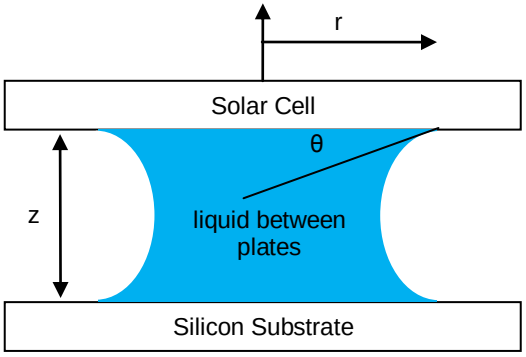

Figure 3 Elements to calculate capillary forces between two parallel plates

$$F = \frac{2\pi\gamma}{z} r^2 \cos\theta \qquad (1)$$

Where:
F is the force experienced between the two parallel plates in N
γ is the surface tension of a liquid in N/m (0.07197 for water)
z is the separation between the two plates in meters
is the radius of the droplet (in this case radius of the cell) in meters
θ is the contact angle (0° was assumed for the worse case wetting scenario)

The formula used to calculate the stress in the anchors due to capillary forces was:

$$\sigma = \frac{F}{wt*\#anchors} \qquad (2)$$

Where :

σ is the stress in the anchors (Pa)
F is the total force experienced by the cell due to capillary forces in N
w is the width of the anchor in m
t is the thickness of the cell or height of the anchor in m
is the number of anchors that attach from the frame to the cell

If the stress was greater than that for yielding in silicon (7GPa), the anchor was assumed to fail. According to these calculations, none of the cell designs with 3 or more anchors, up 1 mm in diameter, with a separation greater than 0.2 µm between the cell and substrate should break due to capillary forces.

Assuming that the cells are fixed at two ends (by anchors) with a distributed force acting on the cell (capillary force), the formula for a beam with fixed ends and a distributed load can be used to calculate the deflection [8]. For the calculations, it was assumed that if the deflection ( ) was greater than the separation between the cell and the substrate, the design would fail by making the cell stick to the substrate.

$$\delta = \frac{Fr^3}{(48)EI} \qquad (3)$$

Where:
δ is the deflection of the beam in meters
F is the total load in Newtons distributed over the length of the cell
r is the radius of the cell
E is the modulus of elasticity. In this case for silicon, 190 GPa
I is the moment of inertia of the cell given by

$$I = \frac{2 \times radius\_cell \times thickness\_cell^{3}}{12} \quad (4)$$

Another restriction included the following: the anchors should be fragile enough to be broken when a piece of tape, with known adhesive force, was attached to the cell. The conditions were calculated with a tape that had an adhesion force of 44 N/100 mm. Then the pulling force per cell was transferred to the anchors to observe whether the stress caused in them was enough to break them. The results obtained were that very small cells (less than 300 µm) would not detach from the anchors.

A range of silicon segment sizes were designed around the optimum calculated value. The designs were an assortment of hexagonal sizes (250, 375, 500, 750, and 1000 µm in diameter). Each segment size design had different anchor characteristics. The number of anchors holding the silicon piece to the handle wafer was 3, 6, 12 or 18. Also, the anchors had different possible positions (corner or edge), and shapes (spring or straight).

A depiction of the layers used to create the masks for the suspended cell using an SOI wafer is shown in Fig. 4. Layer 1 defines a trench which when filled with polysilicon becomes the anchors and their frame. Layer two defines an etch that leaves the cell free from the rest of the frame except where connected with the anchors. It also creates release holes to speed up the release process. Three designs of the anchors were tried: a simple anchor that comes from the center side of the hexagon toward the cell, a simple anchor that comes from the corner of the frame to the corner of the cell, and another one that is "spring like". The section of the simple anchor is smaller where it contacts the cell so it preferably breaks at that point. The spring model attaches to the frame through a "spring like" structure and could be broken easier than the simple anchor since it is less rigid.

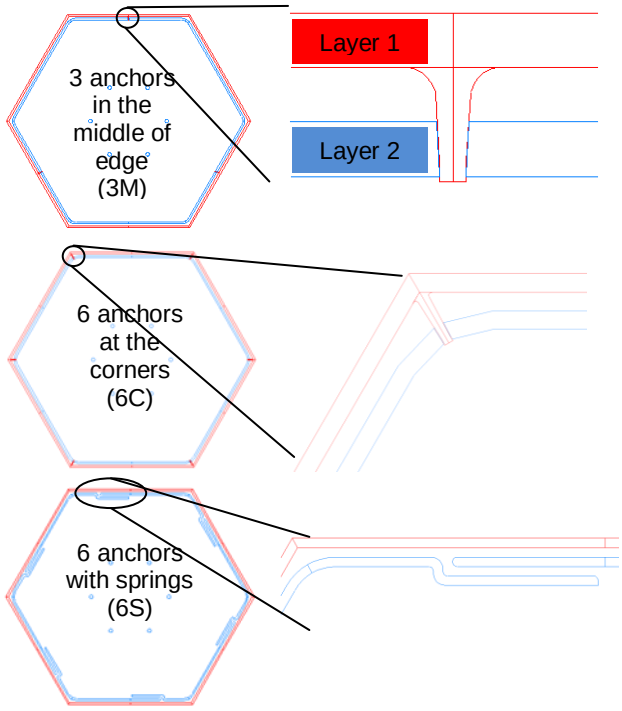

Figure 4. AutoCAD designs for suspended cells

SEGMENTED SILICON SHEET FABRICATION

The fabrication method begins with a silicon-on-insulator (SOI) wafer and uses hydrofluoric acid (HF) chemistry for releasing the suspended silicon structures. Fig. 5 shows cross sections and front views of the process flow used to create the silicon honeycomb structure.

In order to produce these structures, we began by depositing 300 nm of low stress silicon nitride and a 1 µm thick silicon oxide on a 6 inch, 700 µm thick, 2 Ω-cm, SOI, p-type, (100) oriented wafer (Fig. 5A). The wafers were then patterned with 2.2 µm thick photoresist and etched using a deep reactive ion etch process to create 20 µm deep trenches down to the buried oxide (BOX) layer of the SOI wafer forming the shape of the anchors and their frame (Fig. 5B). A wet etch created a cavity in the BOX allowing the anchor to connect to the handle wafer (Fig. 5C). A 2 µm thick poly-silicon layer was deposited to fill the previously fabricated trenches to create both the anchor frame and the anchors (Fig. 5D). The layer deposited was chemi-mechanically polished (CMP) leaving the anchor plugs intact (Fig. 5E). Then, another pattern and deep etch process defined the release holes and the edges of the hexagonal silicon structures. The final etch (Fig. 5F) was performed with a wet etch in a 49% HF solution with Tergitol™ at room temperature for 70 min to suspend the silicon structure by selectively etching the BOX and leaving the silicon intact.

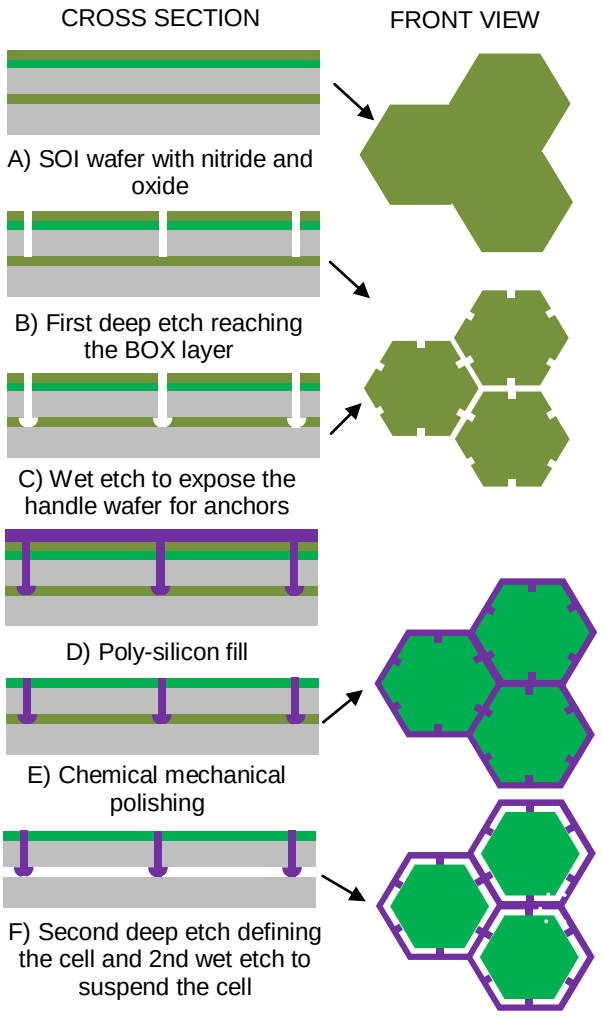

Figure 5 Cross section illustrating the process flow for creation and suspension of the thin silicon sheet.

CHARACTERIZATION

After the structures were fabricated, we evaluated the success rate of different designs in being able to suspend the design (not sticking to the handle wafer) as well as successfully transferring the cells onto tape. Figure 6 shows a section of the die with three sizes: 1mm cell with 12 anchors in the right bottom, 750um in the left and 500um cells in the top. It can be seen that for the 1mm cells with 12 anchors, the capillary forces were enough to make the cell stick to the substrate, This is not desirable because there should be a gap between the cell and the handle wafer so that the nitride layer can be applied during later processing.

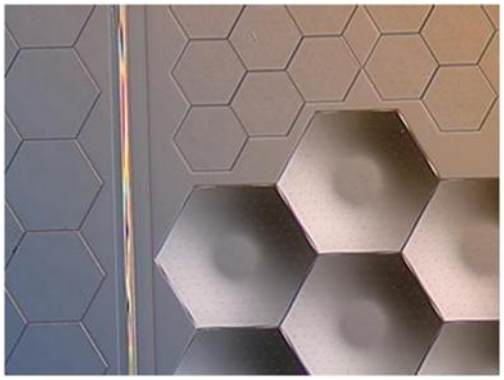

Figure 6 Tape transfer of ultrathin silicon segments.

To detach the cells from the handle wafer, we used a clear adhesive film (1027 from Ultron Systems). This film was also used as the final substrate for the cells. Figure 7 shows a small die with different die sizes transferred onto tape.

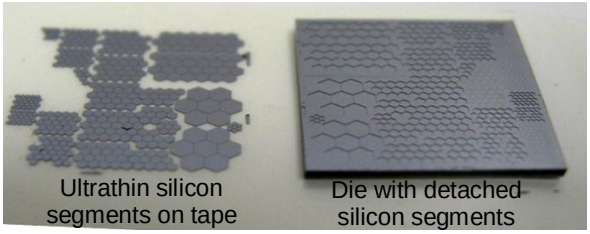

Figure 7 Tape transfer of ultrathin silicon segments.

All designs were successfully suspended except for the 1 mm silicon structures with 12 or less anchors. In the transfer, most of the designs succeeded except the 250 µm structures with more than 3 anchors, and the 375 µm structures with more than 6 anchors. Table 1 summarizes the results.

Table 1. conditions and results of suspended cells

	Number of anchors and Position/shape (C=corner M=middle, MS= middle with spring)					
size (µm)	3 M	6 M	6 M	6 MS	12 M	18 M
250	✓	-	-	✓	-	-
375	✓	✓	-	✓	-	-
500	✓	✓	✓		✓	✓
750		✓			✓	✓
1000					✖	✓

design fabricated design not fabricated

✓ successful (not stuck to handle wafer and transferred to tape)

- means design wasn't stuck due to capillary forces but it was not able to be transferred to tape (anchors were too robust)

✖ means design failed due to capillary forces (stuck to substrate) but was able to be released into tape

After performing transfer tests for the segmented silicon sheet, an experiment was performed to see if a silicon

nitride AR/passivation layer could be deposited in a conformal manner on the front (exposed) and back (hidden) side of the suspended structure while they were still attached to the handle wafer.

LPCVD nitride was used to deposit 85 nm of silicon nitride on the structures using a furnace. Thickness and uniformity were measured for the nitride on the front of the cell (the side facing the wafer) since the quality of the AR properties is dependent on these variables. A NanoSpec 6100 spectral reflectometer (manufactured by Nanometrics), was used to make the measurements. The tool has two separate broadband light sources: a deuterium lamp that measures with UV wavelengths (typically 250-400 nm) and a tungsten halogen lamp that measures with visible wavelengths (typically 480-800 nm). It also has several objectives, which provide for a range of measurement spot sizes from 6 microns to roughly 60 microns. These measurements used visible wavelengths and a spot size of approximately 25 microns. Fig. 8 shows thickness and uniformity of the nitride coating on the back of the silicon pieces.

Fig. 8 reveals that the thickness and uniformity increased as the size of the structure decreased. The inset shows a microscope picture of a 500 µm diameter silicon segment with a color coded bar for nitride thickness. Edges of the structure have a thicker coating and center of the structure is thinnest.

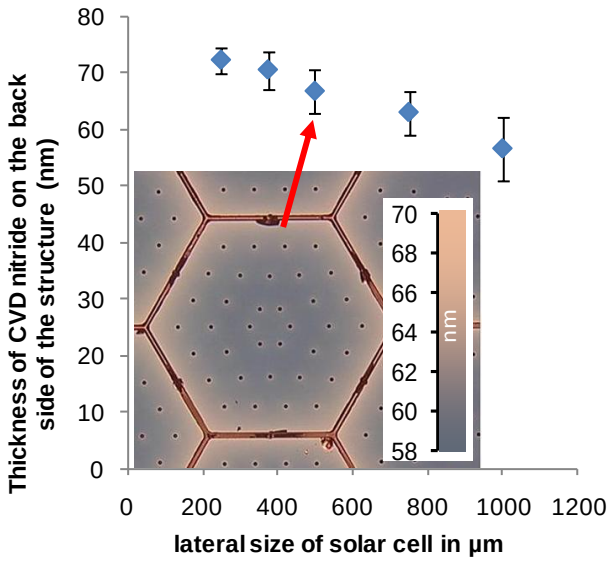

Figure 8 Thickness of nitride on the backside of the die after CVD deposition. Inset shows the back of a 500 µm segment with a color scale for thickness.

Finally, a study was conducted to see the effect of pressure on uniformity of the film as well as the ratio of thicknesses between front and back. Fig. 9 shows both the ratio and standard deviation.

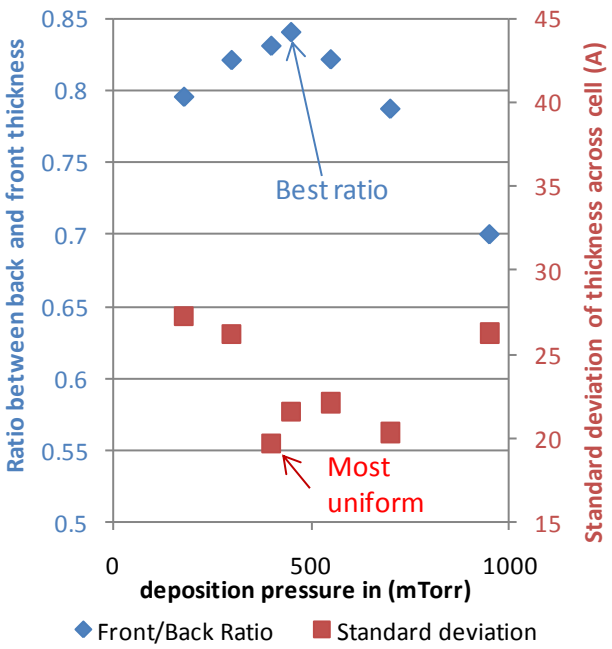

Figure 9 Ratio and uniformity of the nitride coating for different pressures

Blue diamond points in the graph represent average of the thickness on back (side facing handle wafer) divided by the front thickness. Thickness in the back was measured across the cell from one edge of the hexagon to center of the cell while avoiding the release holes. Tool used was the same one described for the measurement shown in Fig. 8. We expected from theory that lower the pressure inside the growth chamber, more uniform the coating in the back will be. However from Figure 9, it can be seen that the uniformity was better (lower standard deviation) for pressures around 400 mTorr where it reaches a maximum. The uniformity decays from there as the pressure is either decreased or increased. We believe that some other process detail related to the tool starts to be significant at pressures below 400 mTorr. Regarding the ratio between thickness in the back and front of the cell, a maximum ratio of 0.83 was reached at a pressure of 450 mTorr.

Finally, a second set of photolithographic masks were designed consisting of 750 µm structures with 12 anchors. With these silicon structures, some prototype flexible silicon sheet demonstration pieces (up to 1.25" X 5" in size) were put together to show the feasibility of this technique for larger areas. Fig. 10 shows a 0.9"X 0.9" (silicon area) ultrathin and flexible silicon sheet.

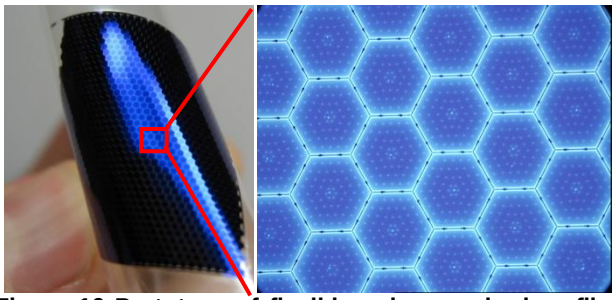

Figure 10 Prototype of flexible solar panel: clear film covered with 20 µm thick segmented crystalline silicon structures.

CONCLUSIONS

We have developed an approach to create ultrathin (<20 µm) and highly flexible silicon sheets that are transferrable to inexpensive substrates. The technology relies on microfabrication tools to create a honeycomb segmented film that is detachable from the wafer through small breakable anchors. Before being transferred to the flexible substrate, the structures received a coating of LPCVD nitride. The measurements show that smaller cells are preferred in order to have a more uniform nitride thickness on the backside. Also, pressures between 400-450 mTorr achieve higher uniformity and better front to back thickness ratios. Finally, a prototype for a flexible solar panel was fabricated showing the feasibility of this technology to create ultrathin sheets of silicon that could be converted into functional solar cells.

REFERENCES

[1] V. Gupta, J. L. Cruz-Campa, M. Okandan, G. N. Nielson, "Microsystems-Enabled Photovoltaics: A Path to the Widespread Harnessing of Solar Energy", *Future Photovoltaics* **1**, (2010) 28-36

[2] J. Yoon, A. J. Baca, S.-I. Park, P. Elvikis, J. B. Geddes Iii, L. Li, R. H. Kim, J. Xiao, S. Wang, T.-H. Kim, M. J. Motala, B. Y. Ahn, E. B. Duoss, J. A. Lewis, R. G. Nuzzo, P. M. Ferreira, Y. Huang, A. Rockett, and J. A. Rogers, "Ultrathin silicon solar microcells for semitransparent, mechanically flexible and microconcentrator module designs", *Nature Materials* **7** (2008) 907 - 915

[3] E. Franklin, V. Everett, A. Blakers, and K. Weber, "Sliver Solar Cells: High-Efficiency, Low-Cost PV", *Techn.Adv. in OptoElectronics* **2007** (2007) 353831-9

[4] G.N. Nielson, M. Okandan, P. Resnick, J.L. Cruz-Campa, T. Pluym, P. Clews, E. Steenbergen, V. Gupta, "Microscale c-Si PV cells for low-cost power", *34th IEEE PVSC* (2009) 1816-1821

[5] G. N. Nielson, M. Okandan, P. Resnick, J. L. Cruz-Campa, P. Clews, M. Wanlass, W. Sweatt, E. Steenbergen, V. Gupta, "Microscale PV cells for concentrated PV applications", *24th EU PVSEC* (2009) 170-173

[6] J. L. Cruz-Campa, M. Okandan, P. J. Resnick, P. Clews, T. Pluym, R.K. Grubbs, V. P. Gupta, D. Zubia, G. N. Nielson, "Microsystems enabled photovoltaics: 14.9% efficient 14 µm thick crystalline silicon solar cell", *Solar Energy Materials and Solar Cells* **95** (2011) 551–558

[7] P. Lambert, Capillary Forces in Microassembly, Springer, USA (2007)

[8] http://www.structsource.com/analysis/types/beam.htm (last accessed in May 2011)